## Supplemental Information

### Supplemental Methods

### Method S1: Characteristic Diffusion time for SCFA in Apical Compartment. Related to Table 1.

The characteristic transient diffusion time is $\tau_D \sim L^2/D_{AB}$, where $D_{AB}$ is the diffusion coefficient. For molecules in the molecular weight range of glucose and SCFA diffusing in culture media or loose mucus, DAB ~0.5-1 x $10^{-5}$ $cm^2/s$) at 37F.
Hence, for L = 0.3 cm (the height of the apical compartment above the epithelial layer, assuming the mucus layer is negligible)
is $\tau_D \sim L^2/D_{AB} \sim (0.3\ cm)^2/(5 \times 10^{-6}\ cm^2/s) = 18{,}000$ s = 5 hr. Thus, butyrate produced in the mucus layer will not saturate the apical flow during its ~0.5 hr transit through the apical compartment.

### Method S2: Glucose diffusion is not limiting the fermentation in *F. prausnitzii* layer. Related to Table 1.

Assumptions:

To estimate how the ~40 μm thickness of the *F. prausnitzii* layer that appears to be embedded in a loose mucus layer above the epithelial barrier (Fig 2), we presume the following:

(i) the microbes are evenly distributed in a mucus layer of L = 40 μm thickness
(ii) no convection in the mucus layer
(iii) culture medium flowing over the top of the mucus layer contains a bulk concentration of glucose $C_{bulk}$ = 2.8 mM ($2.8 \times 10^{-6}$ $mole/cm^3$) as the main precursor for butyrate fermentation
(iv) glucose diffuses into the mucus microbial mass from the bulk in a one dimensional manner and is consumed at a zero-order volumetric rate, which is approximately equal to the production rate of butyrate; this assumption does not directly account for glucose consumed for bacterial growth except through the carbon stoichiometry differences (glucose = 6, butyrate = 4).
(v) the bulk apical medium is the only source of butyrate

Thiele modulus – dimensionless group reflecting ratio of reaction:diffusion

A mass balance on 1 diffusion and with zero reaction in the bacterial mass yields the dimensionless parameter called the Thiele modulus, $F^2$.[116]

$$F^2 = Q_g L^2/(D_g C_{bulk})$$

here $Q_g$ is the volumetric butyrate production rate (measured) and $D_g$ is the diffusion coefficient for glucose in the bacterial mass. For values of $F^2 > 2$, the reaction is strongly diffusion limited as the substrate concentration drops to zero at the far edge of the diffusion/reaction path when $F^2 = 2$. For metabolic reactions, further analysis could be conducted

using first-order or non-linear (e.g. Michaelis-Menten) rate expressions; the Thiele modulus approach is an order-of-magnitude assessment of diffusion limitations.

Data used

(i) The diffusion coefficient of glucose is $1 \times 10^{-6}$ $cm^2/s$.
(ii) Bulk concentration of glucose = 2.8 mM
(iii) Production rate of butyrate = 19 + 1.6 + 0.2 μmol = 22 μmol in 48 hr (data in Table 1).
With L = 40 μm thick layer of mucus/bacteria, $V_{bacteria}$ = 1.1 $cm^2 \times 0.004$ cm = 0.0044 $cm^3$
$Q_g = 2.2 \times 10^{-5}$ mol/0.0044 $cm^3$/48 hr/3600s/hr $= 3.18 \times 10^{-9}$ mole/$cm^3$/s

Analysis

$F^2 = Q_g L^2/(D_g C_{bulk})$
$= (3.18 \times 10^{-9}$ mole/$cm^3$/s)$(0.004cm)^2/(1 \times 10^{-6}$ $cm^2$/s)/$(2.8 \times 10^{-6}$ mol/$cm^3)$
= 0.018
For these conditions, the fermentation reaction is not limited by diffusion of glucose.

**Supplemental figures and legends**

**Figure S1.** Oxygen and shear stress distribution in GuMI physiome platform. (**A**) oxygen distribution in the apical and basolateral sides of colon epithelia after reaching equilibrium. Concentrations on the basolateral side were measured in pilot experiments. Unit in scale bar is kPa. (**B**) Time course of oxygen in apical side. (**C**) top-down view of oxygen concentration distribution in the apical compartment. Unit in scale bar is kPa. (**D**) the volumetric distribution of oxygen concentration reveals 86.6% of the media in the apical compartment is at low oxygen level (<1kPa). Unit in scale bar is kPa. (**E**) distribution of shear stress across the monolayer (top-down view). Unit in scale bar is MPa. (**F**) Shear stress distribution. (**G**) side view and (**H**) top-down view of the simulation for the flow streamline. Unit in scale bar in (G-H) is mm/s. Related to Figure 2.

**Figure S2.** Bright field images of the monolayer cultured under Static (A), GuMI (B), and GuMI-FP (C). bar scale = 300 μm. (**D-E**) Representative images of different epithelial cell types (colonocytes and goblet cells) in Static conditions. (**F**) Concentration of short chain fatty acids in effluent from in GuMI-NB and GuMI-FP after 48 h of co-culturing. Related to Figure 2.

**Figure S3.** Overview of the effects of GuMI and *F. prausnitzii* on the gene expression of colon epithelial cells. (**A**) volcano plot of the genes in GuMI vs Static, the significantly changed genes are highlighted in green; total n is the number of genes with TPM > 0 in all samples, sig. n is the number of genes that are significantly changed (adj. $p<0.05$, log2FoldChange>0.5). (**B**) volcano plot of the significantly changed genes in GuMI+FP vs GuMI, the significantly changed genes are highlighted in red; (**C**) Overlap on the genes changed by GuMI and *F. prausnitzii*. The number in the circle indicates the number of genes changed uniquely by only either condition or by both conditions. The chromosol distribution of the changed genes in GuMI vs Static(**D**) and GuMI+FP vs GuMI (**E**). (**F**) Heatmap of the core genes that are significantly under-represented in NB, and the function of these genes in DNA replication machinery for pre-initiation, initiation, elongation, and maturation of DNA. MCM: DNA helicase family minichromosomal maintenance protein complex; CDC: cell division cycle protein; GINS2, GINS Complex Subunit 2; POLA1-2, DNA polymerase alpha 1 and 2; POLD3, DNA polymerase delta 3; PCNA, proliferating cell nuclear

antigen; RFC, replication factor C subunit; ORC, origin recognition complex subunit; LIG1: DNA ligase. Related to Figure 3.

**Figure S4.** Transcriptional changes of HIF1A related genes in GuMI vs Static and TLR related genes in GuMI-FP vs GuMI-NB. (**A**) No significant changes of HIF1A negative regulator genes EGLN1, EGLN2, EGLN3, HIF1AN in GuMI-NB vs Static. NB/ST: GuMI-NB/Static. Related to Figure 4 (**B**) Changes of TLR3 and TLR4 and their downstream genes in GuMI-FP vs GuMI-NB. Related to Figure 5.

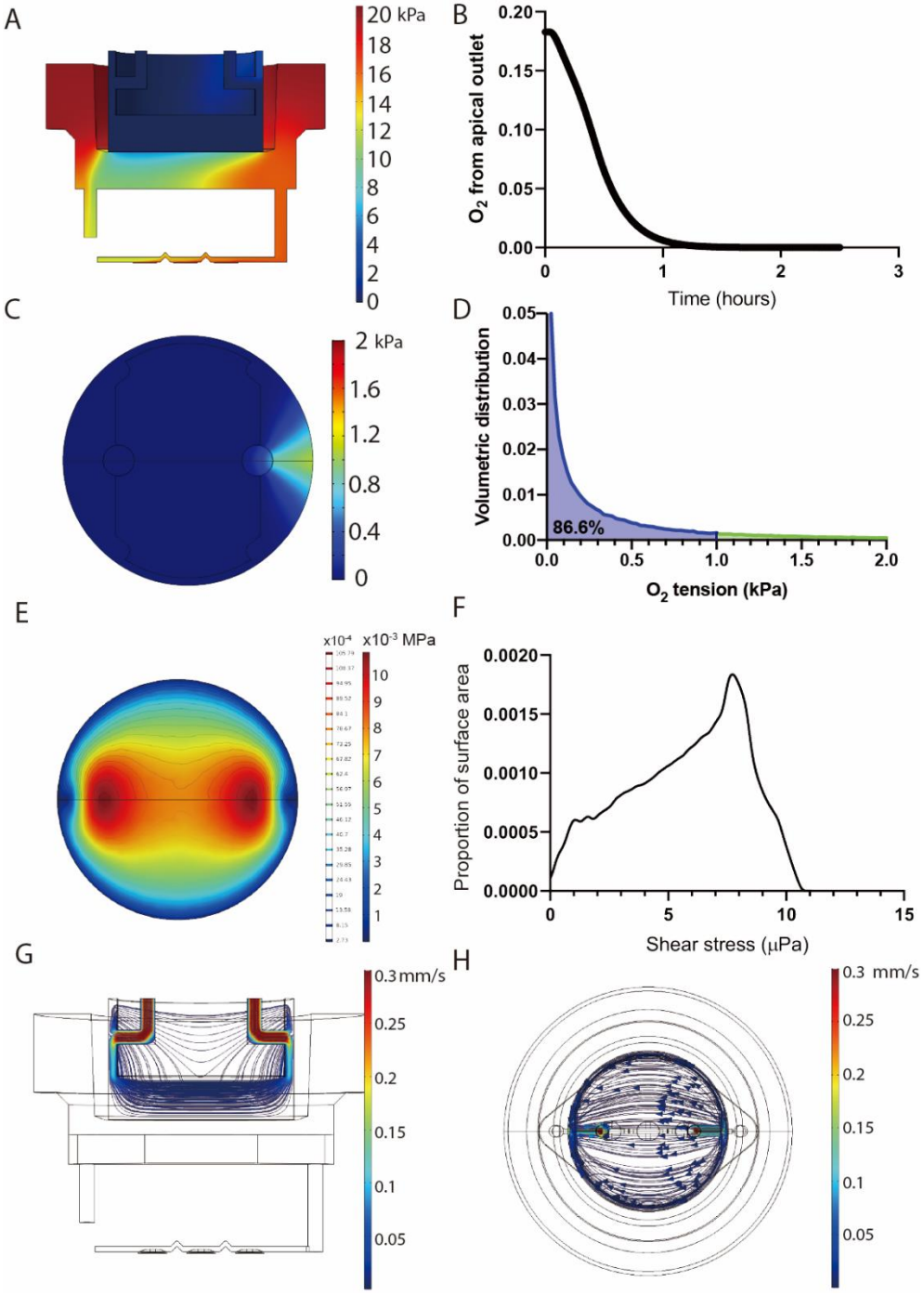
A
20 kPa
18
16
14
12
10
8
6
4
2
0
B
$O_2$ from apical outlet
0.20
0.15
0.10
0.05
0.00
0
1
2
3
Time (hours)
C
2 kPa
1.6
1.2
0.8
0.4
0
D
Volumetric distribution
0.05
0.04
0.03
0.02
0.01
0.00
86.6%
0.0
0.5
1.0
1.5
2.0
$O_2$ tension (kPa)
E
x10⁻⁴
x10⁻³ MPa
10
9
8
7
6
5
4
3
2
1
F
Proportion of surface area
0.0020
0.0015
0.0010
0.0005
0.0000
0
5
10
15
Shear stress (μPa)
G
0.3 mm/s
0.25
0.2
0.15
0.1
0.05
H
0.3 mm/s
0.25
0.2
0.15
0.1
0.05

**Figure S1.**

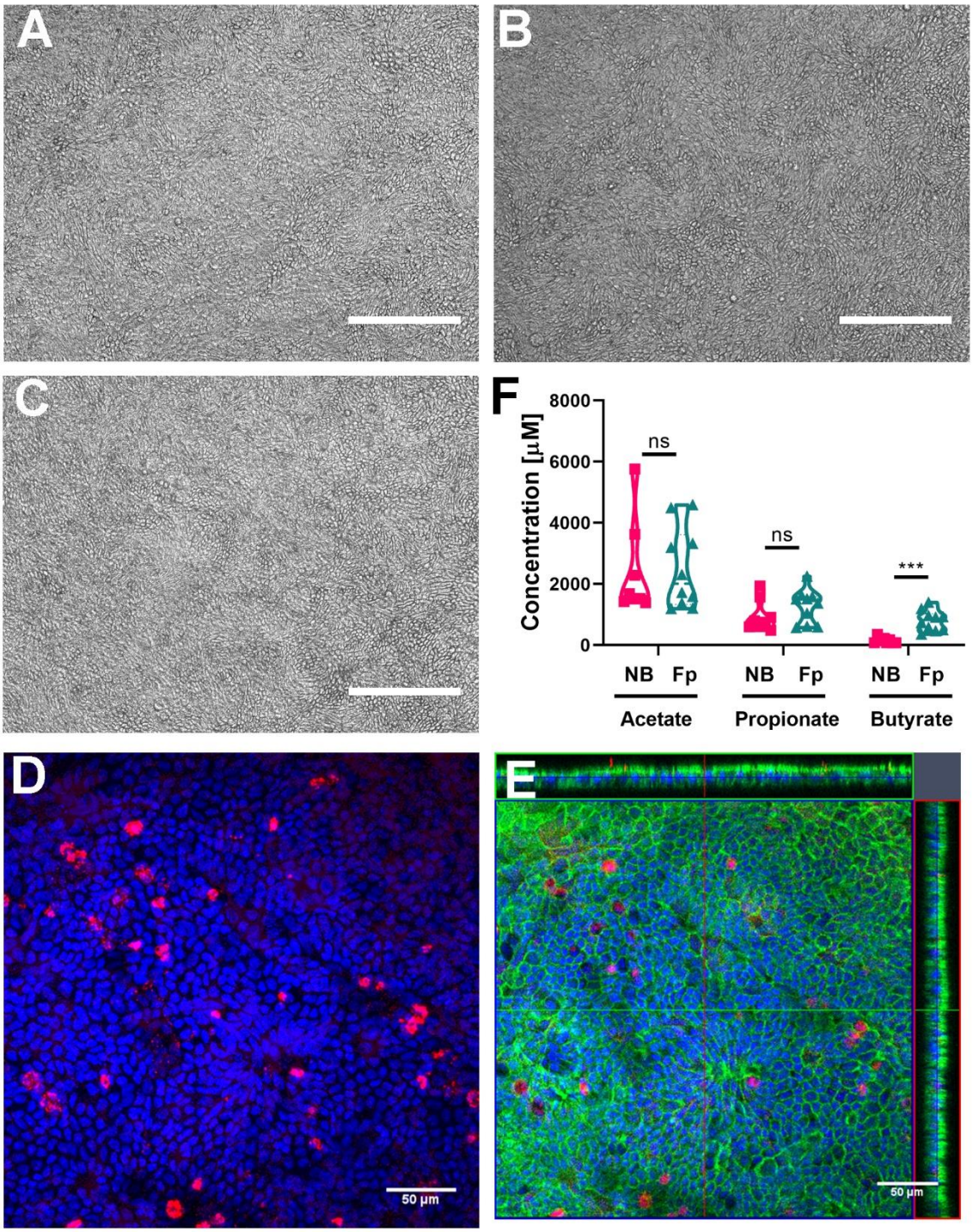
A
B
C
D
E
F
Concentration [µM]
8000
6000
4000
2000
0
ns
ns
***
NB
Fp
NB
Fp
NB
Fp
Acetate
Propionate
Butyrate
50 µm
50 µm

**Figure S2.**

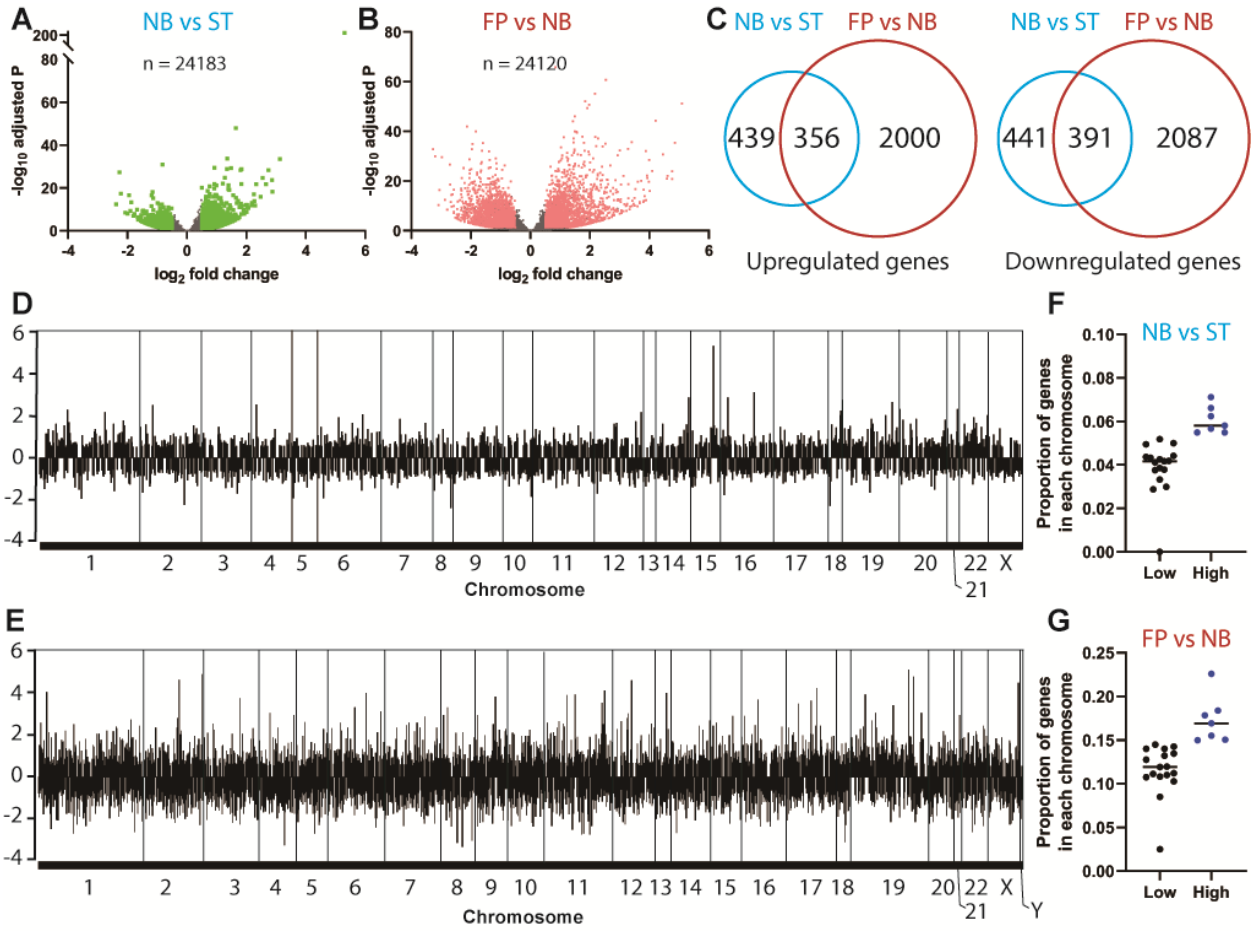
A
NB vs ST
n = 24183
-log10 adjusted P
log2 fold change
B
FP vs NB
n = 24120
-log10 adjusted P
log2 fold change
C
NB vs ST
FP vs NB
439
356
2000
Upregulated genes
NB vs ST
FP vs NB
441
391
2087
Downregulated genes
D
Chromosome
1 2 3 4 5 6 7 8 9 10 11 12 13 14 15 16 17 18 19 20 21 22 X
E
Chromosome
1 2 3 4 5 6 7 8 9 10 11 12 13 14 15 16 17 18 19 20 21 22 X Y
F
NB vs ST
Proportion of genes in each chromosome
Low
High
G
FP vs NB
Proportion of genes in each chromosome
Low
High

**Figure S3.**

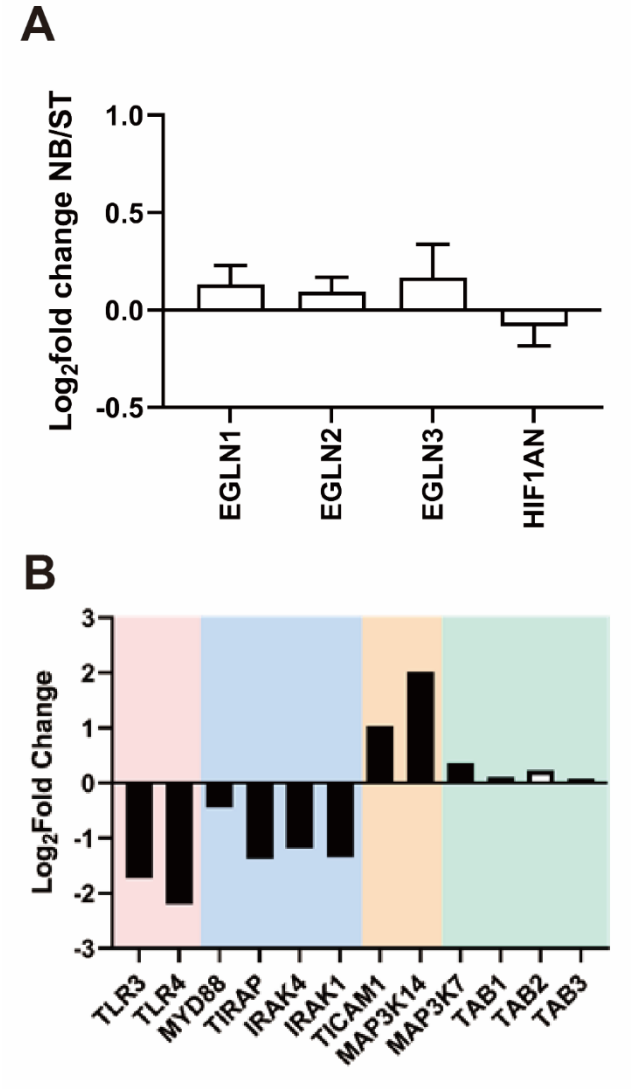
A
Log2fold change NB/ST
1.0
0.5
0.0
-0.5
EGLN1
EGLN2
EGLN3
HIF1AN
B
Log2Fold Change
3
2
1
0
-1
-2
-3
TLR3
TLR4
MYD88
TIRAP
IRAK4
IRAK1
TICAM1
MAP3K14
MAP3K7
TAB1
TAB2
TAB3

**Figure S4.**